Received: 12 June 2020 | Revised: 22 November 2020 | Accepted: 26 November 2020

DOI: 10.1002/hbm.25310

RESEARCH ARTICLE

WILEY

# Probing the role of the right inferior frontal gyrus during Pain-Related empathy processing: Evidence from fMRI and TMS

Yun Li[1,2] | Wenjuan Li[1] | Tingting Zhang[1] | Junjun Zhang[1] | Zhenlan Jin[1] | Ling Li[1]

[1]MOE Key Lab for Neuroinformation, High-Field Magnetic Resonance Brain Imaging Key Laboratory of Sichuan Province, Center for Psychiatry and Psychology, School of Life Science and Technology, University of Electronic Science and Technology of China, Chengdu, China

[2]School of Management, Chengdu University of Traditional Chinese Medicine, Chengdu, China

**Correspondence**
Ling Li, Key Laboratory for NeuroInformation of Ministry of Education, High-Field Magnetic Resonance Brain Imaging Key Laboratory of Sichuan Province, Center for Information in Medicine, School of Life Science and Technology, University of Electronic Science and Technology of China, Chengdu, China, 610054.
Email: liling@uestc.edu.cn

**Funding information**
National Natural Science Foundation of China, Grant/Award Number: 61773092; 61673087; 61773096; Sichuan Science and Technology Program, Grant/Award Number: 2020YFS0230; The Open Project of Sichuan Applied Psychology Research Center from Chengdu Medical College, Grant/Award Number: CSXL-192A09; The Scientific Research of Sichuan Health Commission, Grant/Award Number: 19PJ193

## Abstract

Recent studies have suggested that the right inferior frontal gyrus (rIFG) may be involved in pain-related empathy. To verify the role of the rIFG, we performed a functional magnetic resonance imaging (fMRI) experiment to replicate previous research and further designed a noninvasive repetitive transcranial magnetic stimulation (rTMS) experiment to probe the causal role of the rIFG in pain-related empathy processing. We assigned 74 volunteers (37 females) to three groups. Group 1 ($n$ = 26) performed a task in which participants were required to perceive pain in others (task of pain: TP) and we used fMRI to observe the activity of the rIFG during pain-related empathy processing. Then, we applied online rTMS to the rIFG and the vertex site (as reference site) to observe the performance of Group 2 ($n$ = 24; performing TP) and Group 3 ($n$ = 24; performing a control task of identifying body parts; task of body: TB). fMRI experiment demonstrated stronger activation in the rIFG than in the vertex during the perception of pain in others ($p < .0001$, Bonferroni-corrected). rTMS experiment indicated that when the rIFG was temporarily disrupted, participants perceived pain in others significantly more slowly ($p < .0001$, Bonferroni-corrected) than when the vertex was disrupted. Our results provide evidence that the rIFG is involved in pain-related empathy processing, which yields insights into how the brain perceives pain in others.

**KEYWORDS**

empathy, functional magnetic resonance imaging, pain, repetitive transcranial magnetic stimulation, right inferior frontal gyrus

## 1 | INTRODUCTION

Empathy is a broad concept that refers to the vicarious sensing and understanding of another person's perceptual and emotional experience (Coll et al., 2017). As a complex psychological construct, a variety of negative and positive feelings have been used as targets for the study of empathy, such as pain, disgust, and happiness (Chakrabarti, Bullmore, & Baron-Cohen, 2006; Dimberg, Andréasson, & Thunberg, 2011; Jabbi, Swart, & Keysers, 2007; Jackson, Meltzoff, & Decety, 2005; Loggia, Mogil, & Catherine Bushnell, 2008;

Morelli, Rameson, & Lieberman, 2014; Rymarczyk, Zurawski, Jankowiak-Siuda, & Szatkowska, 2016; Silva, Montant, Ponz, & Ziegler, 2012; Singer et al., 2004). Pain is one of the core components of human suffering. Thus, empathy for pain is fundamental to social interaction. People who show less empathy for pain, as well as those who are too sensitive to others' pain, may not be socially well-adapted (Gallo et al., 2018; Young, Gandevia, & Giummarra, 2017).

The existence of two systems of empathy is acknowledged: the cognitive empathy system and the emotional empathy system. Cognitive empathy is a cognitive role-taking process that involves adopting another's point of view and understanding another's perspective (Shamay-Tsoory, 2011; Shamay-Tsoory, Aharon-Peretz, & Perry, 2009). Converging evidence from neuroimaging and lesion studies has shown that a neural network that includes the medial prefrontal cortex, the temporoparietal junction, and the medial temporal lobes is necessary for cognitive empathy (De Waal & Preston, 2017). On the other hand, emotional empathy involves the ability to resonate with other people's mental and physical states (e.g., perceiving another person's feelings, recognition of the emotion, and affectively reacting to these observed feelings) (Shamay-Tsoory, 2011; Shamay-Tsoory et al., 2009). Human neuroimaging studies of pain-related empathy have shown that merely observing someone else in pain (based on observable perceptual cues or contextual information) elicits an emotional empathic response (Decety & Lamm, 2006;Bernhardt & Singer, 2012;Lamm, Rütgen, & Wagner, 2019). According to the perception–action model (Preston & Waal, 2002), emotional empathic responses might activate one's own representations for the direct experience of pain automatically when observing pain in others, and the output from this shared representation automatically proceeds to motor areas of the brain where responses are prepared. This state-matching response is related to the activation of a network that includes the anterior/middle cingulate cortex and the anterior/middle insula cortex, which have been reported to respond to both felt and observed pain (Fan, Duncan, de Greck, & Northoff, 2011; Lamm, Decety, & Singer, 2011; Timmers et al., 2018).

In addition, the "human mirror neuron system" (hMNS) is thought to provide the neural mechanism for embodied simulation in social cognition (e.g., empathy) (Gallese, 2007) and might be particularly well-suited to provide the state-matching mechanism involved in emotional empathy (De Waal & Preston, 2017). The inferior frontal gyrus (IFG) has been theorized to be one of the core regions of the hMNS (Bernhardt & Singer, 2012; Betti & Aglioti, 2016; Gallese, 2007; Hillis, 2014), which demonstrates hemispheric asymmetry in the simulation mechanism. The left IFG has been associated with semantic and phonological processing (Liakakis, Nickel, & Seitz, 2011), action observation, and imitation (Hamzei et al., 2016). The right IFG (rIFG) might be an overlap region for social cognitive, emotional, and interoceptive (related to the sense of the physiological condition of the body) processes (Adolfi et al., 2017). In terms of pain-related empathy processing, previous studies (Budell et al., 2010a; Budell, Kunz, Jackson, & Rainville, 2015) have found that the perception of pain-related signals (through facial expressions of pain) and the extraction of their meaning to infer the state of the expresser were associated with stronger activation of the rIFG. The rIFG may be involved in emotion recognition (through emotional-communicative information, such as facial expressions) and conversion of the observed facial expressions of pain into a pattern of neural activity that would enable the observer to infer the state of the expresser, thus providing the neural basis for emotional empathy. In line with these observations, non-pain facial expression-based empathy necessitates the activity of the rIFG, as revealed by a recent cortical stimulation study (Wu et al., 2018). However, a few studies have also found that, when participants focused on pain using objective cues about the sensory component of the observed pain (e.g., pain in limbs), the rIFG also demonstrated stronger activation (Grèzes, Armony, Rowe, & Passingham, 2003; Iacoboni, 2005; Iacoboni, 2009; Vachon-Presseau et al., 2012). These results might indicate that the rIFG may be involved in understanding the meaning of pain-related visual cues. Nevertheless, no study to date has examined the involvement of the rIFG in pain-related empathy through objective sensory cues of the observed pain.

From the above studies, it is clear that the rIFG plays a significant role in brain mechanisms that underlie empathy for pain. However, most of the above results were obtained from imaging studies. Recently, noninvasive brain stimulation methods, such as transcranial magnetic stimulation (TMS)/transcranial direct current stimulation (tDCS), have come to be used widely to detect brain–behavior interactions (Valero-Cabré, Amengual, Stengel, Pascual-Leone, & Coubard, 2017). A recent tDCS study provided evidence for the role of the rIFG in empathy activated by non-pain facial expressions (Wu et al., 2018). Nevertheless, imaging methods merely detect associations between activation of a certain brain region and behavior. Furthermore, the spatial resolution of tDCS is lower than that of TMS (Keeser et al., 2011), which makes it difficult to obtain causal evidence of brain–behavior interactions (Filmer, Dux, & Mattingley, 2014). Therefore, the current study used TMS to investigate whether the rIFG is involved in pain-related empathy processing based on objective sensory cues of the observed pain. To the best of our knowledge, no previous study has explored the role of the rIFG in pain-related empathy via TMS.

First, we conducted an fMRI experiment using a pain-related empathy-induction task (task of pain: TP) and sought to replicate previous findings about empathy in the pain network. Because the rIFG is a heterogeneous gyral complex, whose subregions may differ in morphology and cell structure (Dricu & Frühholz, 2016), we used the fMRI experiment to determine the specific location of the rIFG for subsequent TMS experiments. We assumed that the response of the rIFG would be much more intense when healthy participants perceive pain in others. Then, we applied online repetitive TMS (rTMS) at 10 Hz, to probe the functional roles of the rIFG in pain-related empathy. In the rTMS experiment, two groups of participants performed a TP or task of body (TB). In TP, participants viewed images of others in painful or neutral situations and indicated whether the person shown in the image was suffering pain. In the TB, participants viewed the same images of others and were instructed to judge whether the body part shown in the image was a hand or a foot. Based on a previous study,

these two tasks were matched in difficulty (Gu, Liu, Dam, Hof, & Fan, 2013). The TP requires more explicit pain-related empathy processing resources than the TB, as confirmed by Gu et al. (Gu et al., 2013). The contrast between the TP and TB might reflect differences in pain-related emotional demand. While no relevant rTMS studies on pain-related empathy have provided reference stimulation parameters, a recent meta-analysis found that rTMS stimulation applied at 10 Hz might disrupt the accuracy or slow the response time (RT) for tasks involving cognitive processing (Beynel et al., 2019). We hypothesized that rTMS stimulation at 10 Hz might impair participants' performance in perceiving other people's pain.

## 2 | MATERIALS AND METHODS

### 2.1 | Participants

Seventy-five healthy volunteers (right-handed) were recruited from the University of Electronic Science and Technology of China (UESTC). Participants were randomly assigned to three groups. Group 1 (27 healthy volunteers) participated in the fMRI experiment. One participant was removed from the analysis due to a high amount of errors (> 40%, some of which involved lack of response) during the task; consequently, 26 individuals eventually participated in the fMRI experiment. Group 2 (24 healthy volunteers) and Group 3 (24 healthy volunteers) participated in the rTMS experiment. To characterize the participants of this study and to ensure that the experimental groups did not differ with respect to relevant empathy traits, self-reported trait empathy (see details in Section 2.2) was assessed for each participant. As shown in Table 1, the groups did not differ significantly in terms of the gender ratio and trait empathy. Although the participants in Group 1 were older than those in Group 2, there was no significant difference in age between Groups 2 and 3. All participants had normal or corrected-to-normal visual acuity and normal color vision, with no previous history of head injury, neurological problems, prolonged pain, diagnosed psychiatric disorders, or regular medication of any kind. None of the participants had any magnetic objects in the body or any other contraindication to fMRI and TMS experiments. Each participant provided written informed consent prior to participation in accordance with the principles expressed in the Declaration of Helsinki (World Medical Association, 2013). The study was approved by the Institutional Review Board of UESTC MRI Research Center. All procedures were in accordance with the recommendations of UESTC's guidelines for human behavior studies.

### 2.2 | Measures of empathy characteristics

Before the experiment, participants completed the Chinese version (Zhang, Dong, Wang, Zhan, & Xie, 2010) of the Interpersonal Reactivity Index (IRI) questionnaire (Davis, 1983) in a quiet testing room, using the Wenjuanxing website (https://www.wjx.cn/), to measure the participants' trait empathy. The Chinese version of the IRI (IRI-C) has been demonstrated to have satisfactory reliability and validity (Gao et al., 2017; Jiang et al., 2014; Zhang et al., 2010). The IRI-C is a self-reported questionnaire that assesses both cognitive and affective components of trait empathy, using four subscales: (a) the perspective taking scale (PT), reflecting a tendency to understand and adopt another's psychological point of view spontaneously (e.g., agreeing with the statement "I sometimes try to understand my friends better by imagining how things look from their perspective"); (b) the fantasy scale (FS), reflecting a tendency to imaginatively transpose oneself into fictional situations (e.g., agreeing with the statement "When I watch a good movie, I can very easily put myself in the place of a leading character"); (c) the empathic concern scale (EC), reflecting other-oriented feelings of warmth, compassion, and concern in response to others' states (e.g., agreeing with the statement "I am often quite touched by things that happen"); and (d) the personal distress scale (PD), reflecting self-oriented feelings of distress, anxiety, discomfort or personal unease in response to others' states (e.g., agreeing with the statement "When I see someone who badly needs help in an emergency, I go to pieces"). The PT and FS subscales measure the cognitive component of trait empathy, while the EC and PD subscales reflect the affective component. Participants answered the above items on a 5-point Likert scale (1 = strongly disagreed, 5 = strongly agreed). Higher scores on the PT, FS, EC, and PD subscales are associated with higher trait empathy. Cronbach's alpha for the IRI-C in this study was 0.854.

**TABLE 1** Demographic characteristics and self-reported measures (mean values ± *SEM*) for each group and *p*-value for the effect of Group

| | Group 1 | Group 2 | Group 3 | F/$\chi$2 | *p* value | Post hoc *t* test |
|---|---|---|---|---|---|---|
| Age | 22.77 ± 0.41 | 21.21 ± 0.42 | 22.04 ± 0.37 | 3.835 | .026 | Group 1 > 2[a] |
| Gender (M/F) | 14/12 | 10/14 | 13/11 | 0.987 | .610 | |
| IRI-C-PT | 3.60 ± 0.08 | 3.46 ± 0.08 | 3.76 ± 0.09 | 2.932 | .06 | |
| IRI-C-EC | 3.78 ± 0.09 | 3.72 ± 0.09 | 3.83 ± 0.09 | 0.317 | .729 | |
| IRI-C-FS | 3.42 ± 0.11 | 3.42 ± 0.16 | 3.55 ± 0.13 | 0.325 | .723 | |
| IRI-C-PD | 3.20 ± 0.12 | 2.93 ± 0.12 | 3.01 ± 0.11 | 1.364 | .262 | |

Abbreviations: EC, empathic concern scale; F, female; FS, fantasy scale; IRI-C, the Chinese version of the interpersonal reactivity index; M, male; PD, personal distress scale; PT, perspective taking scale.

[a]$p < .05$ Bonferroni corrected.

## 2.3 | Experimental stimuli

The experimental materials used in this study were digital color photographs showing another person's hand or foot in painful or neutral situations, and were selected from a subset of homemade experimental materials. The models used in these images were all Chinese. The "painful" situation depicted various incidents occurring in everyday life, such as a hand or a foot cut by scissors, trapped in a door, injured by a hammer, and so forth. A "neutral" situation depicting a hand or foot in similar but innocuous situations served as the control condition for nonspecific attention and visual processes. We selected 72 photographs (18 photographs in each of the four categories: painful-foot, painful-hand, neutral-foot, neutral-hand) for the fMRI experiment and the rTMS experiment (see Figure 1a). An independent group of 45 college students rated the degree of pain expressed in the images on a 9-point scale from 1 (not painful at all) to 9 (extremely painful). The pain ratings of painful and neutral photographs (mean values ± *SEM*: 6.89 ± 0.14 and 1.14 ± 0.03, respectively) were significantly different ($t$[44] = 21.696, $p$ < .0001). We selected photographs scoring higher than 7 points or lower than 2 points for the experiment. Neutral images were selected based on their pain counterparts, but with scores of <2 points. Additionally, 2 × 2 repeated-measures analysis of variance (ANOVA; with Bonferroni-correction) was performed for rating data with body part (hand/foot) and picture valence (painful/neutral) as the within-subject factors. There was a significant main effect of picture valence ($F$(1, 17) = 1853.378, $p$ < .0001, $\eta_p^2$ = 0.991). There was no significant main effect of body part ($F$(1, 17) = 1.471, $p$ = .242, $\eta_p^2$ = 0.080), and there was no significant picture valence × body part interactions ($F$(1, 17) = 0.652, $p$ = .431, $\eta_p^2$ = 0.037). The painful foot images were not rated as significantly more painful than the painful hand images (painful foot: 7.02 ± 0.15 vs. painful hand: 6.76 ± 0.21; $t$[17] = 1.012, $p$ = .326). The neutral hand images were not rated as significantly more neutral than the neutral foot images (neutral hand: 1.11 ± 0.02 vs. neutral foot: 1.15 ± 0.02; $t$[17] = −1.290, $p$ = .214). All photographs were edited to the same size (640 × 480 pixels) and were identical in context, size, background, brightness, contrast, and other physical properties.

## 2.4 | fMRI procedure

We presented 72 stimuli in a mini-blocked fMRI design following Kao's instructions (Kao, 2014). The participants were instructed on how to perform the experimental task and were successful in a brief training session (36-trial practice) prior to entering the scanner. The stimuli used in the practice session were not used in the fMRI experiment. Then, subjects participated in two sequential fMRI runs; each run consisted of 18 blocks and 2 conditions (painful/neutral). Each block consisted of four 4-s trials of the same condition (fixation screen = 200 ms, target screen = 750 ms, reaction screen = 3,050 ms).

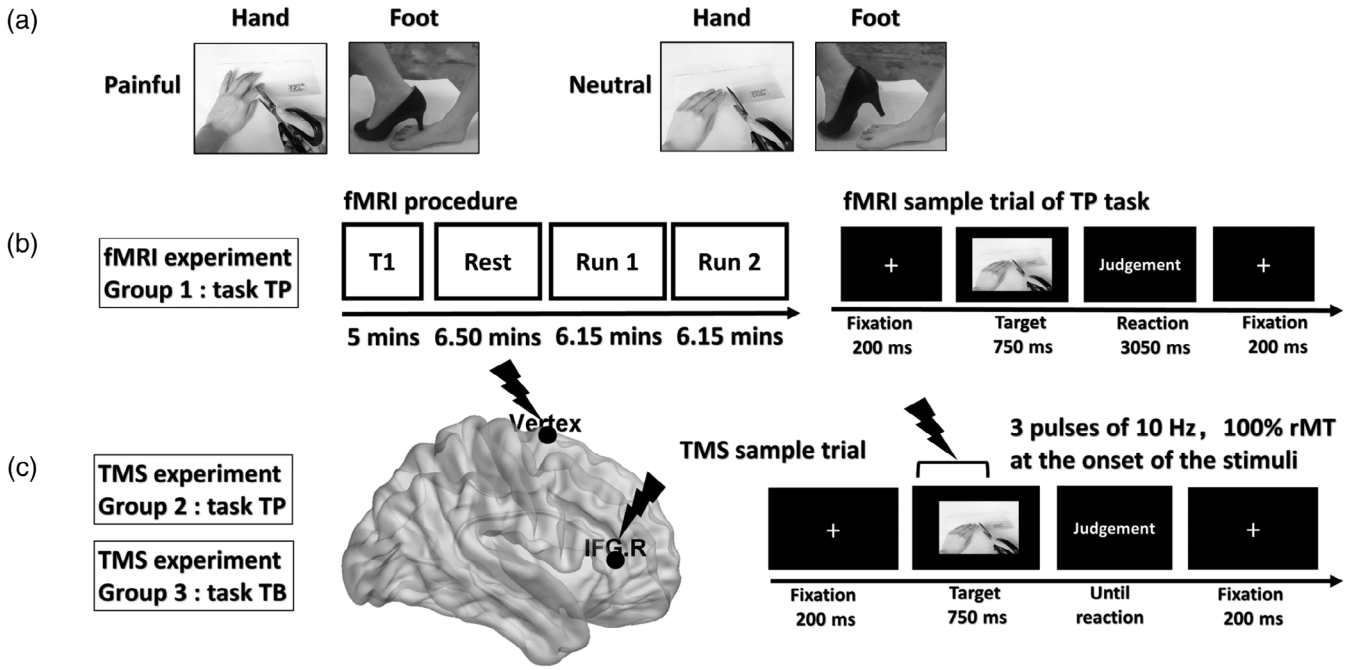


**FIGURE 1** Sample stimuli, experiment sample trial, and procedure. (a) Representative example of the stimuli used in the current study: digital photographs showing another person's hand or foot in painful or neutral situations. (b) fMRI procedure and sample trial. Participants (Group 1) viewed images of others in painful or neutral situations and indicated whether the person shown in the image was suffering pain (TP). (c) rTMS procedure and sample trial. Group 2 performed a pain-related empathy task (TP). Group 3 performed a body part identification task (TB). During the performance of the task (TP or TB), participants in both Group 2 and Group 3 were given two sessions (vertex and rIFG) of rTMS stimulation in a randomized order. rTMS, repetitive transcranial magnetic stimulation; rIFG, right inferior frontal gyrus; fMRI, functional magnetic resonance imaging; TP, task of pain; TB, task of body

The order of the conditions/blocks was random. We inserted a blank screen of 5 s between each block of trials and a 30-s fixation period at the end of each session to allow skin conductance (Bach, Flandin, Friston, & Dolan, 2010) and hemodynamic responses (Friston, Frith, Turner, & Frackowiak, 1995) to return to baseline. We instructed participants to feel and judge whether the person shown in the image was suffering from pain, as quickly and accurately as possible, by pressing one of two designated buttons on a response box, using a pain-related empathy-induction task (TP) (see Figure 1b) adapted from the paradigm used in previous studies (Gu et al., 2013; Gu et al., 2015). The complete scanning process took 12.3 min. After scanning, participants rated the intensity of pain supposedly felt by the person in the stimulus image on a 9-point scale (1 = not painful at all, 9 = extremely painful).

## 2.5 | fMRI data acquisition and preprocessing

All participants underwent fMRI scanning in a 3.0-T GE DISCOVERY MR750 scanner (General Electric Medical Systems, Milwaukee, WI) at the UESTC laboratory. Functional MR images were acquired with a gradient echo planar imaging (EPI) sequence, with the following scanning parameters, as in our previous study (Zhang et al., 2019): TR = 2000 ms, TE = 30 ms, flip angle = 90°, matrix size = 64 × 64, voxel size = 3.75 × 3.75 × 3 $mm^3$, 43 slices. After a 6.5-min resting-state fMRI scan, we acquired high-resolution whole-brain volume T1-weighted images obliquely with a 3D spoiled gradient echo pulse sequence (TR = 5.932 ms, TE = 1.956 ms, flip angle = 9°, matrix size = 256 × 256, FOV = 25.6 × 25.6 $cm^2$, and slice thickness = 1 mm) to control for any anatomic abnormalities and to increase normalization accuracy during preprocessing.

We performed fMRI image preprocessing using SPM12 (Statistical Parametric Mapping; Wellcome Trust Centre for Neuroimaging, London, UK, http://www.fil.ion.ucl.ac.uk/spm), implemented in MATLAB R2013a (MathWorks, Sherborn, MA). The first five EPI volumes of the fMRI images were discarded for signal stabilization. fMRI data preprocessing included slice-timing correction, three-dimensional motion correction, co-registration to individual anatomical images, normalization to the Montreal Neurological Institute (MNI) reference space (3 × 3 × 3 $mm^3$), and spatial smoothing with an 8-mm Gaussian kernel (full-width at half-maximum). Imaging in all participants met the standards of total vector motion <1.5 mm and rotation <1.5°.

## 2.6 | fMRI data analysis: Task effects and activity of ROIs

We computed a first-level analysis using the general linear model for each subject via vectors corresponding to the onset of the target screen series (duration set to 0) and collapsed across two task conditions (painful/neutral), with a hemodynamic response function modeled as a boxcar function. In addition, six motion parameters were added to the design matrix. At the single-subject level, contrasts were then calculated to establish the hemodynamic correlates of task conditions (task painful/neutral > fixation baseline). A paired *t* test was used to evaluate different activations between the two task conditions (painful-neutral and neutral-painful). At the group level, whole brain multi-subject analysis was subsequently assessed by submitting the individual SPMs to a one-sample *t* test using a random-effects model (Forman et al., 1995). We applied whole-brain voxelwise false discovery rate (FDR) correction ($p < .005$, cluster size >70 voxels) to control for false positives.

We selected the rIFG and the vertex (as control site) as regions-of-interest (ROIs) according to multisubject statistical contrast maps (painful-neutral). We drew a 6-mm-radius sphere (centered on the peak activation of each cluster) using the MarsBaR toolbox (http://marsbar.sourceforge.net), and extracted the fMRI activation beta values (parameter estimates) of the ROIs. We selected the rIFG and the vertex (as control) for the following TMS experiment. Because the context of empathy for pain might modulate the functional connectivity between the seed regions (the rIFG, the middle cingulate cortex and the insular cortex (Carrillo et al., 2019; Fan et al., 2011; Hutchison, Davis, Lozano, Tasker, & Dostrovsky, 1999; Lamm et al., 2011; Shackman et al., 2011; Timmers et al., 2018)) and other brain regions, separate generalized psychophysiological interaction (gPPI; https://www.nitrc.org/projects/gppi) analyses (McLaren, Ries, Xu, & Johnson, 2012) were performed using the above seeds (see Supplemental Materials for details).

## 2.7 | TMS design and site localization

The study used a 2 (Stimulation Site: vertex vs. rIFG) × 2 (Picture Valence: painful stimuli vs. neutral stimuli) × 2 (TMS group: Group 2 vs. Group 3) design. The stimulation site and picture valence were within-subject factors, and the rTMS group was the between-subject factor. Participants from Group 2 performed the TP, which was adapted from the empathy-for-pain paradigm used by Gu et al. (Gu et al., 2015). In the TP, participants viewed images of others in painful or neutral situations and indicated whether the person shown in the image was suffering pain. Group 3 performed a body-part (i.e., foot or hand) identification task (TB) as a control task, also adapted from Gu et al. (Gu et al., 2013). In the TB, participants viewed the same images of others as in the TP, but were instructed to judge whether the body part shown in the image was a hand or a foot. These two tasks were matched in difficulty (Gu et al., 2013). The TP requires more explicit pain-related empathy processing resources than the TB, as confirmed by Gu et al. (Gu et al., 2013). The contrast between the TP and TB might reflect differences in pain-related emotional demand.

Figure 1c illustrates an example trial of the TP and TB. Each trial commenced with the presentation of a fixation cross for 200 ms, followed by (a) a target-displaying phrase (750 ms); (b) a judgment phrase: participants were instructed to choose between "neutral" and "painful" for the TP or between "hand" and "foot" for the TB, as quickly and accurately as possible by pressing the "F" or "J" button (counterbalanced between participants). When the participants reacted, the trial ended, and the next trial began. The order of stimuli

was pseudorandomized. Each participant underwent two sessions of rTMS stimulation at the vertex (a control site) and rIFG. Each session contained 216 trials. Each of the 72 stimuli was shown three times. Participants were given a self-paced break every 72 trials. The experimental stimuli were presented at a distance of 60 cm and were displayed in the center of a Dell monitor with a resolution of 1,024 × 768 pixels and a refresh rate of 60 Hz. E-prime 2.0 (Psychology Software Tools, Sharpsburg, PA) was used for the stimulus presentation, the recording of the behavioral results, and the generation of rTMS triggering.

During the performance of the task, online rTMS was delivered at 10 Hz in trains of three pulses (300-ms long) at the site of stimulation, using a Magstim super rapid magnetic stimulator and an air-cooled figure-of-eight coil with an outer winding diameter of 70 mm (Magstim Company Limited, Whiteland, United Kingdom). The onset of TMS pulses coincided with the appearance of the target stimuli. Each participant received 216 × 3 pulses for each TMS site.

A 3.0-T GE Sigma scanner acquired high-resolution anatomical T1-weighted MR images of all participants. The scanner parameters were the same as in the fMRI experiment. The stimulation locations were targeted via the BrainSight stereotaxic neuronavigator (Rogue Research, Montreal, QC, Canada), equipped with a Polaris Vicra position sensor system. The location of the coil was determined by the anatomical data imported into the neuro-navigation software and was used for stereotaxic co-registration of the participant's brain with the TMS coil.

We applied online rTMS at the vertex and the rIFG. We selected the vertex as a control site for providing the same sound and the same scalp sensation, but without interfering with ongoing task-related activity (Jung, Bungert, Bowtell, & Jackson, 2016). For stimulation over the vertex, the TMS coil was positioned at the MNI coordinates 0, 0, 80, which was localized as the midpoint of a region halfway between the nasion and the inion, and equidistant from the left and right ear (He, Fan, & Li, 2017; Yan, Wei, Zhang, Jin, & Li, 2016). For stimulation over the rIFG, the TMS coil was based on the reference coordinate (x = 48, y = 36, z = 6) obtained from the activation peak in the fMRI experimental group effect analysis (Figure 2).

The resting motor threshold was identified immediately before the delivery of rTMS. It was established as the lowest stimulation intensity of single-pulse TMS stimulation that had a 50% chance (5 of 10 pulses) to evoke motor potentials exceeding 50 μV (peak-to-peak amplitude) in the target muscle (contralateral first dorsal interosseous muscle) following stimulation over the left-hand area of the participant's right motor cortex at rest. The online rTMS stimulation intensity corresponded to 100% of the resting motor threshold. For Group 2, the rTMS intensity ± *SEM* for the vertex and the rIFG was 41.42% ± 0.95 of the maximum stimulator output. For Group 3, the rTMS intensity ± *SEM* for the vertex and the rIFG was 42.19% ± 0.66 of the maximum stimulator output. Mean stimulation intensities did not differ between Group 2 and Group 3 (comparison: $t[46] = -0.665$, $p = .510$).

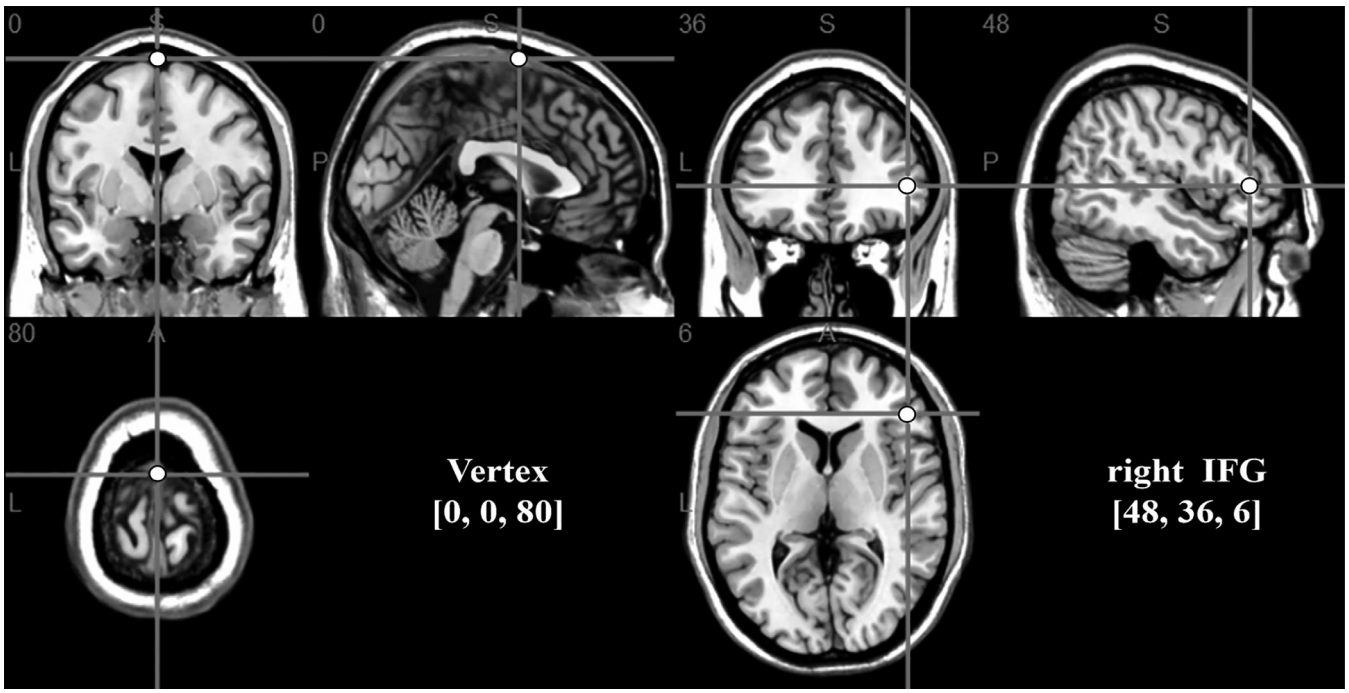


**FIGURE 2** TMS locations. Coronal, axial, and sagittal views of the stimulated site depicted on a standard template from MRIcro. For the stimulation over the vertex (control site), the TMS coil was positioned at the following MNI coordinates: 0, 0, 80, which was localized as the midpoint of the region halfway between the nasion and the inion, and equidistant from the left and right ears. For stimulation over the rIFG site, the TMS coil was based on the reference coordinate (x = 48, y = 36, z = 6) obtained from the activation peak of the fMRI in experimental group effect analysis. MNI, Montreal Neurological Institute; TMS, transcranial magnetic stimulation; rIFG, right inferior frontal gyrus; fMRI, functional magnetic resonance imaging

Participants took part in a 1-hr rTMS experiment in which both vertex and rIFG sites were stimulated. First, the participant completed the IRI-C trait empathy questionnaires. Then, the experimenter explained the task requirements in detail. Participants next performed a practice of TP or TB tasks. The stimuli used in the practice session were not shown in the rTMS experiment. After this, each participant's motor threshold was established. Then, participants in both Group 2 and Group 3 were given two sessions (vertex and rIFG) of rTMS stimulation in a randomized order. After the rTMS experiment, the experimenter questioned the participants about the discomfort caused by the active TMS. Participants reported no discomfort or adverse effects, and the experimenter did not notice any such effects. Then, participants rated the intensity of pain supposedly felt by the person in the images on a 9-point scale (1 = not painful at all, 9 = extremely painful). Participants rated the painful stimuli significantly higher than the neutral stimuli (7.69 ± 0.12 and 1.31 ± 0.08, respectively; $t$[47] = 45.423, $p$ < .0001), validating the significance of their affective content. We did not observe any significant gender differences in adjusted RTs or pain-rating scores (see Table S2 for summary statistics and $t$ tests in detail).

## 2.8 | fMRI and TMS behavioral data analysis

IBM SPSS Statistics 21.0 (IBM, New York, NY) was used for analysis of all behavioral data. We first calculated each participant's IRI-C scores. We checked linearity assumptions, and calculated summary statistics and correlations between each subscale. As previous studies have reported gender differences on the IRI, we also performed independent samples $t$ tests between our male and female participants for each subscale. In addition, RTs and correct response rates (accuracy) in fMRI and rTMS experiments were measured. Trials were rejected if they had an incorrect response or lacked a button press between 200 and 1,200 ms after the onset of the stimulus array. The behavioral results are presented as the mean values ± *SEM*, unless otherwise mentioned. We also analyzed gender differences in the behavioral results and the relationships between the activity of ROIs and trait empathy scores or behavioral measures, by using Pearson correlation analysis. All significance tests were two-tailed, and significant $p$-values were set at .05. Repeated-measures ANOVA (with Bonferroni-correction) was performed on rTMS behavioral data with the stimulation site and picture valence as within-subject factors, and TMS group as a between-subject factor. We performed Pearson's correlation analysis between the TMS behavioral results and the trait empathy scores.

# 3 | RESULTS

## 3.1 | Trait empathy

As our experiment was a mixed-design experiment, to ensure homogeneity of groups and facilitate comparison of our results with previous studies on empathy, we checked linearity assumptions and calculated summary statistics and correlations between each IRI-C subscale. As shown in Tables 1 and 2, the IRI-C subscale scores had a normal distribution and were consistent with previously reported norms (Davis, 1980). We did not observe any significant differences in the mean scores on the PT, EC, FS, or PD subscales among the three groups (comparison: $F_{PT}$ (2, 71) = 2.932, $p$ = .06; $F_{EC}$ (2, 71) = 0.317, $p$ = .729; $F_{FS}$ (2, 71) = 0.325, $p$ = .723; $F_{PD}$ (2, 71) = 1.364, $p$ = .262). Additionally, as previously reported (Allen et al., 2017), the FS ($t$[72] = 1.989, $p$ = .05) and PD subscale ($t$[72] = 3.294, $p$ = .002) scores were greater in females than in males. Moreover, we found that scores on the PT subscale correlated positively with those on the EC ($r$ = .498, $p$ < .0001) and FS subscales ($r$ = .366, $p$ = .001). Scores on the EC subscale correlated positively with those on the FS ($r$ = .555, $p$ < .0001) and PD subscales ($r$ = .330, $p$ = .004). Moreover, scores on the FS subscale correlated positively with those on the PD subscale ($r$ = .312, $p$ = .007). All correlations were Bonferroni-corrected at $\alpha$ = .05.

## 3.2 | fMRI task effects: Behavioral data

We measured RTs and accuracy during fMRI scanning. The accuracy for painful and neutral conditions was 93.08 ± 1.08% and 92.42 ± 1.34%. Because accuracy exceeded 90% in all the experimental conditions, the mean RT adjusted for accuracy (adjusted RT for each participant = raw RT/proportion of correct responses) was calculated to account for any possible trade-off between speed and accuracy (Bona, Herbert, Toneatto, Silvanto, & Cattaneo, 2014; Pasalar, Ro, & Beauchamp, 2010). The results revealed no significant difference in adjusted RT between the painful and neutral conditions (768.59 ± 24.06 and 794.12 ± 29.23, respectively; $t$[25] = −1.508, $p$ = .144). Ratings of the pictures presented after the fMRI sessions indicated that participants rated the painful stimuli as significantly more painful than the neutral stimuli (8.00 ± 0.14 and 1.13 ± 0.05, respectively; $t$[25] = 42.144, $p$ < .0001), thus validating the significance of their affective content. We did not observe any significant gender differences in adjusted RTs or pain rating scores (see Table 3 and Table S1 for summary statistics and $t$ tests in detail).

## 3.3 | fMRI task effects: Whole-brain analysis

We performed whole-brain functional analysis, comparing painful conditions and neutral conditions (contrast analysis: painful > neutral). Table 4 shows all the areas in which the signal was significantly associated with painful stimulus processing for Group 1 (FDR corrected $p$ < .005, cluster size >70). As expected, increased activation of the painful stimuli as compared with neutral stimuli was found in the rIFG (peak coordinates: x = 48, y = 36, z = 6; $t$ = 4.70, $p_{[FDR\ corrected]}$ = .001, cluster size = 82, see Figure 3a). The rIFG responded to painful stimuli more strongly than to the neutral stimuli. Other painful (as opposed to neutral) stimuli yielding peaks of significant changes in activity were found in the left insula, the left mid-cingulate cortex, the bilateral

**TABLE 2** IRI-C descriptive statistics

| | IRI-C-PT | IRI-C-EC | IRI-C-FS | IRI-C-PD |
|---|---|---|---|---|
| Total number of subjects | 74 | 74 | 74 | 74 |
| Gender (male/female) | 37/37 | 37/37 | 37/37 | 37/37 |
| Minimum | 2.86 | 2.86 | 2.00 | 1.80 |
| Maximum | 4.57 | 4.71 | 4.83 | 4.20 |
| Mean ± *SEM* | 3.60 ± 0.05 | 3.78 ± 0.05 | 3.46 ± 0.08 | 3.05 ± 0.07 |
| Skewness | 0.177 | 0.050 | 0.026 | 0.346 |
| *SE* of Skewness | 0.279 | 0.279 | 0.279 | 0.279 |
| Kurtosis | −0.837 | −0.649 | −0.724 | −0.751 |
| *SE* of kurtosis | 0.552 | 0.552 | 0.552 | 0.552 |
| Kolmogorov–Smirnov Z | 0.956 | 0.793 | 0.885 | 1.331 |
| *p*-value (two-tailed) | .320 | .555 | .414 | .058 |
| Male (mean ± *SEM*) | 3.64 ± 0.07 | 3.70 ± 0.08 | 3.31 ± 0.10 | 2.84 ± 0.09 |
| Female (mean ± *SEM*) | 3.57 ± 0.07 | 3.86 ± 0.08 | 3.61 ± 0.11 | 3.26 ± 0.09 |
| *t* test (*df* = 72) | 0.645 | −1.506 | −1.989 | −3.294 |
| *p*-value (two-tailed) | .521 | .136 | .05 | .002 |

Abbreviations: EC, empathic concern scale; FS, fantasy scale; IRI-C, the Chinese version of the interpersonal reactivity index; PD, personal distress scale; PT, perspective taking scale.

**TABLE 3** Behavioral data of fMRI experiment (Mean values ± *SEM*)

| | Accuracy (%) | RTs (ms) | Adjusted RTs | Rating scores |
|---|---|---|---|---|
| Painful (*N* = 26) | 93.08 ± 1.08 | 714.15 ± 22.31 | 768.59 ± 24.06 | 8.00 ± 0.14 |
| Neutral (*N* = 26) | 92.42 ± 1.34 | 729.73 ± 23.13 | 794.12 ± 29.23 | 1.13 ± 0.05 |
| *t* test (*df* = 25) | 0.579 | −1.476 | −1.508 | 42.144 |
| *p*-value (two-tailed) | .568 | .152 | .144 | <.0001 |

occipital visual areas, cerebellum, and the parietal lobes, which have been found to be significantly associated with pain-related empathy in previous studies (Vachon-Presseau et al., 2012).

Based on group activation of the whole-brain contrast analysis (painful > neutral), we determined the ROIs for the rIFG and vertex, which served as the reference for the rTMS experiment. The selected rIFG was defined as the site of maximal activation in the dorsal and anterior frontal cortex of the right hemisphere including the pars triangularis (BA45) (Hartwigsen, Neef, Camilleri, Margulies, & Eickhoff, 2019). The selected control site (vertex [0, 0, 80]) was defined as the midpoint in the area halfway between the nasion and the inion and equidistant from the left and right ears (Ferrari, Schiavi, & Cattaneo, 2018). We extracted the mean parameter estimates of each selected ROI (rIFG and Vertex) for each of the task conditions (painful/neutral). Two-way repeated ANOVA (2 ROIs × 2 task conditions) analysis showed a significant main effect of ROI ($F(1, 25) = 4.446$, $p = .045$, $\eta_p^2 = 0.151$), a marginally significant main effect of task condition ($F(1, 25) = 3.270$, $p = .083$, $\eta_p^2 = 0.116$), and a significant ROI (rIFG/vertex) × task condition (painful/neutral) interaction ($F(1, 25) = 26.044$, $p < .0001$, $\eta_p^2 = 0.510$). Based on the significant interaction effect, data were stratified by condition (painful/neutral) to examine how painful emotion can affect different ROIs within the pain-related empathy processing network. We used a paired *t* test, Bonferroni-corrected for multiple comparisons, to identify the source of this two-way interaction (see Figure 3b). We found that the rIFG was more active in the painful condition than in the neutral condition ($t[25] = 4.380$, $p < .0001$, significant following Bonferroni-correction). In contrast to the rIFG, no difference in the mean beta-value in the vertex was detected between the two task conditions ($t[25] = -0.547$, $p = .589$) was detected between the two task conditions. Although not significant after Bonferroni correction, the rIFG was more active than the vertex ($t[25] = 2.831$, $p < .009$) in the painful condition. Since the beta weights (parameter estimates) were significantly greater in the painful condition than in the neutral condition, an activation difference was obtained by subtracting the neutral parameter estimates from the painful parameter estimates. Then, the mean parameter estimate differences in the rIFG were significantly different from those in the vertex ($t[25] = 5.103$, $p < .0001$, Bonferroni-corrected, see Figure 3c).

Next, we performed correlation analysis to evaluate the relationships between the activity of the rIFG and trait empathy scores (measured by the IRI-C) or behavioral measures. Although the results showed no significant correlation between the activity of the rIFG and behavioral measures ($p > .05$), the mean parameter estimates of the rIFG in the painful condition were marginally significantly positively correlated with the PD scores ($r = .367$, $p = .077$). No other correlation was found.

**TABLE 4** Whole-brain analysis: Stimulus effects for pain-related empathy processing

| Cluster | Brain region | BA | MNI coordinates | | | Local peak *t* score |
|---|---|---|---|---|---|---|
| | | | x | y | z | |
| Cluster analysis corrected for the whole brain: Painful > neutral | | | | | | |
| 2,266 | Postcentral gyrus | 4 | −33 | −27 | 51 | 9.55 |
| 407 | Cerebellum (IV–V) | 37 | 15 | −51 | −24 | 9.02 |
| | Cerebellum (VIII) | 37 | 12 | −72 | −42 | 6.00 |
| 288 | Inferior temporal gyrus | 37 | 45 | −60 | −12 | 6.12 |
| | Inferior occipital gyrus | 19 | 42 | −69 | −9 | 5.94 |
| 608 | Inferior occipital gyrus | 37 | −39 | −60 | −9 | 5.59 |
| | Middle occipital gyrus | 18 | −30 | −90 | 15 | 5.42 |
| 148 | Insula cortex | 48 | −42 | −3 | 12 | 5.14 |
| 89 | Middle cingulate cortex | 24 | −6 | 0 | 39 | 4.29 |
| **82** | **Inferior frontal gyrus pars triangularis** | **45** | **48** | **36** | **6** | **4.70** |
| Cluster analysis corrected for the whole brain: Neutral > painful | | | | | | |
| 4,331 | Precentral gyrus | 4 | 36 | −24 | 57 | 14.36 |
| | Supplementary motor area | 4 | 9 | −24 | 51 | 6.80 |
| 365 | Cerebellum (IV-V) | 37 | −15 | −51 | −21 | 9.97 |
| 73 | Superior occipital gyrus | 18 | 18 | −90 | 18 | 4.82 |
| 134 | Angular gyrus | 39 | 48 | −57 | 39 | 4.43 |

*Note:* MNI, the Montreal Neurological Institute coordinates, which reflect the peak of each cluster, not the centroid. Regions included were thresholded by default at $p < .005$, FDR corrected.
Abbreviation: BA, Brodmann area.

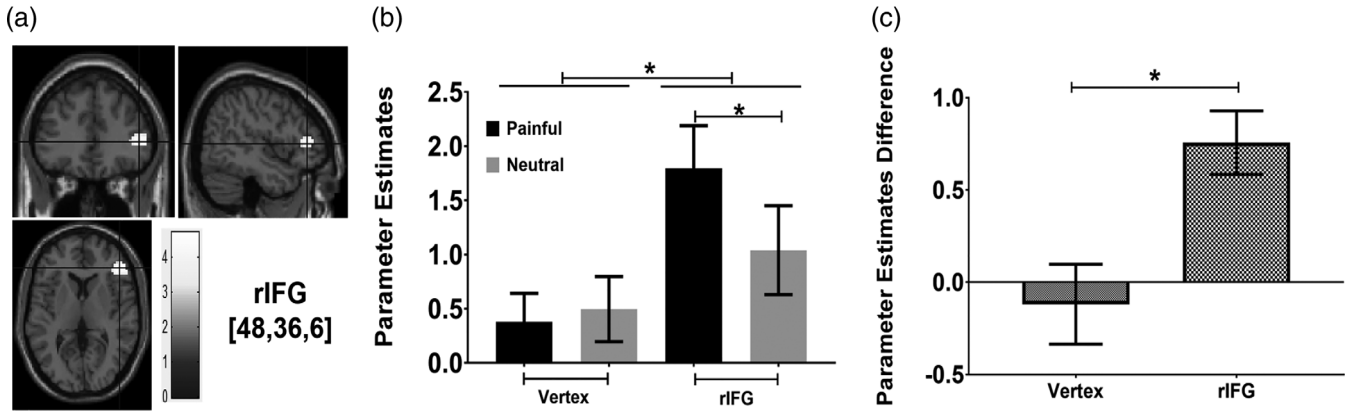


**FIGURE 3** fMRI activation results. (a) The rIFG clusters were significantly activated under the painful condition, as compared with the neutral condition. (b) Beta weights (parameter estimates) extracted from the vertex and rIFG for each of the task conditions (painful/neutral). (c) Beta weights difference (activation difference) obtained by subtracting the neutral parameter estimates from the painful parameter estimates are shown at different ROIs (vertex and rIFG). Errors bars indicate the *SE* of the mean, and asterisks mark Bonferroni correction for multiple comparisons (*$p < .05$). rIFG, right inferior frontal gyrus; fMRI, functional magnetic resonance imaging; ROIs, regions-of-interest

## 3.4 | TMS-induced changes

The mean RT adjusted for accuracy was calculated (listed in Table 5). Three-way repeated-measures ANOVA (Bonferroni-corrected: 2 Stimulation Site × 2 Picture Valence × 2 TMS Group) revealed a nonsignificant main effect of stimulation site ($F(1, 46) = 0.603$, $p = .442$, $\eta_p^2 = 0.013$), a marginally significant main effect of picture valence ($F(1, 46) = 3.102$, $p = .085$, $\eta_p^2 = 0.063$), a nonsignificant stimulation site × TMS group interactions ($F(1, 46) = 2.520$, $p = .119$, $\eta_p^2 = 0.052$), and a nonsignificant picture valence × TMS group interactions ($F(1, 46) = 2.077$, $p = .156$, $\eta_p^2 = 0.043$).

However, there were significant two-way interactions between stimulation site and picture valence ($F[1, 46] = 10.928$, $p = .002$, $\eta_p^2 = 0.192$). Post hoc *t* tests showed that the adjusted RTs were significantly prolonged only after rTMS stimulation over the rIFG in the painful condition ($t[47] = 2.374$, $p = .022$, marginally significant

**TABLE 5** Mean values ± *SEM* of adjusted RTs in rTMS experiment

| | | Group 2 (TP) | | Group 3 (TB) | |
|---|---|---|---|---|---|
| **rTMS site** | **Picture valence** | **Mean** | **SEM** | **Mean** | **SEM** |
| Vertex | Painful | 680.66 | 18.60 | 615.90 | 11.59 |
| | Neutral | 684.20 | 19.22 | 608.92 | 9.80 |
| rIFG | Painful | 740.80 | 37.22 | 602.13 | 8.51 |
| | Neutral | 680.26 | 31.47 | 603.41 | 8.25 |
| Adjusted RT difference of vertex | | −3.54 | 14.28 | 6.98 | 4.36 |
| Adjusted RT difference of rIFG | | 60.53 | 22.68 | −1.29 | 6.23 |

Abbreviations: rIFG, right inferior frontal gyrus; rTMS, repetitive transcranial magnetic stimulation; RTs, reaction times; TB, task of body; TP, task of pain..

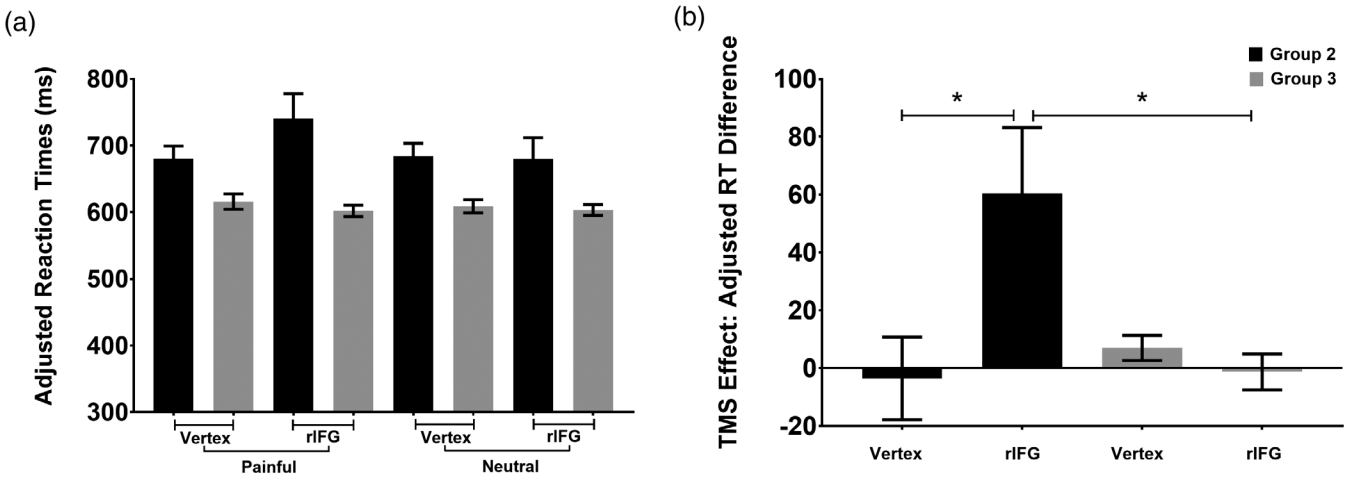


**FIGURE 4** TMS results. (a) Adjusted RTs of two groups for painful and neutral conditions are shown across different stimulation sites. (b) The adjusted RT difference between painful and neutral conditions (subtracting the neutral adjusted RTs from the painful adjusted RTs) of the two groups are shown at different stimulation sites. Error bars show the *SE* of the mean, and asterisks mark significant post hoc *t* test results after Bonferroni-correction for multiple comparisons (*$p < .05$). RT, reaction time

following Bonferroni-correction). More importantly, we observed a three-way interaction of stimulation site × picture valence × TMS group ($F[1, 46] = 18.363$, $p < .0001$, $\eta_p^2 = 0.285$). To identify the source of this three-way interaction, we defined a TMS effect measure as the adjusted RT difference between painful and neutral conditions (by subtracting the neutral adjusted RTs from the painful adjusted RTs). Consequently, the three-way interaction was simplified to a two-way interaction (see Table 5 and Figure 4) between the stimulation site and TMS group ($F[1, 46] = 18.363$, $p < .0001$, $\eta_p^2 = 0.285$). Further simple effects analysis (Bonferroni-corrected) indicated that, while Group 2 (TP: 60.53 ± 22.68) showed a larger adjusted RT difference than Group 3 (TB: −1.29 ± 6.23) under rIFG stimulation ($F(1, 46) = 6.91$, $p = .012$, $\eta_p^2 = 0.131$), no significant group difference was observed for vertex stimulation ($F(1, 46) = 0.497$, $p = .484$, $\eta_p^2 = 0.011$; Group 2 vs. Group 3 = −3.54 ± 14.28 vs. 6.98 ± 4.36). Moreover, stimulating the rIFG (60.53 ± 22.68) resulted in a larger adjusted RT difference than stimulating the vertex (−3.54 ± 14.28) in Group 2 (TP: $t[23] = 4.132$, $p < .0001$, significant following Bonferroni-correction), while no significant stimulation site difference was observed for Group 3 (task TB, $t[23] = -1.239$, $p = .228$; rIFG vs. vertex = −1.29 ± 6.23 vs. 6.98 ± 4.36). Furthermore, we conducted a Pearson correlation analysis between TMS behavior outcomes and trait empathy scores and found a significant negative relationship ($r = -.416$, $p = .043$) between the trait cognitive empathy scores (on the FS subscale) and the adjusted RTs during stimulation of the rIFG in the painful condition, in Group 2 (TP). There was no significant correlation ($r = -.293$, $p = .165$) between the FS scores and the adjusted RTs in the neutral condition during stimulation of the rIFG in Group 2 (TP). There was also no significant correlation between the adjusted RTs and the trait empathy scores for both conditions under vertex stimulation ($p > .05$). Similarly, there was no significant correlation ($p > .05$) between the adjusted RTs and the trait empathy scores in both conditions during stimulation of the rIFG or vertex in Group 3 (TB). Thus, FS subscale scores were lower and adjusted RTs were slower in the painful condition when stimulating the rIFG in Group 2 (TP), indicating that the scores on the FS subscale may be predictive of the effects of rTMS on cognitive empathy.

## 4 | DISCUSSION

The purpose of the current study was to use fMRI and rTMS to investigate whether the rIFG is likely to be involved in pain-related empathy processing. Evidence from fMRI and rTMS data indicate direct involvement of the rIFG during pain-related empathy processing.

In the present fMRI experiment, the rIFG demonstrated stronger activation than that in the vertex during the perception of pain in others. This greater rIFG activation seen during the perception of pain in others was significant only when the neutral trials were excluded from the whole-brain functional analysis (contrast analysis: painful > neutral). Indeed, previous imaging studies and meta-analysis studies revealed that perceiving the pain of others was correlated with activity in the rIFG (Saarela et al., 2007; Hartwigsen et al., 2019; Smallwood et al., 2013;Lamm et al., 2011b;Bzdok et al., 2012). Furthermore, in terms of the location of the peak in the present fMRI study, we observed that BA 45 (the pars triangularis) was located in the anterior portions of the rIFG. The IFG is a heterogeneous gyral complex and its subregions differ in morphology, cellular architecture, and function, implying that its subregions might play various roles (Dricu & Frühholz, 2016). Through coactivation-based parcellation, a recent study delineated cortical clusters in the rIFG (BA 44 and BA 45) and found that the rIFG might be characterized by a posterior-to-anterior axis, with BA 45 mostly located in the anterior part and BA 44 mostly located in the posterior part of the rIFG (Hartwigsen et al., 2019). Hartwigsen et al. found that anterior clusters of the rIFG were associated with higher-level social cognition and emotion than the posterior rIFG (Hartwigsen et al., 2019). Adolfi et al. further reported an overlap of social cognitive processing, such as empathy processing and attribution of cognitive and affective mental states in others, in the anterior portions of the rIFG (BA 45; the pars triangularis) (Adolfi et al., 2017). The results of the present fMRI study provided further imaging evidence for the contribution of the rIFG (BA 45; the pars triangularis) and replicated previous imaging findings about pain-related empathy processing.

In our subsequent rTMS experiments, when the rIFG function was temporarily disrupted by rTMS stimulation, participants were unable to perform the pain-related empathy task rapidly, resulting in prolongation of the adjusted RTs under the painful condition. In the present study, pain in others was perceived as pain of body limbs (i.e., objective cues about the sensory component of the observed pain). This result supports the hypothesis that the rIFG may be involved in pain-related empathy through pain-related sensory cues. Moreover, in the present rTMS experiment, two different tasks were used to direct attention toward either the pain communicated via body limbs (TP) or the visual cues of the body limbs (TB). However, rTMS stimulation only interfered with the participants' performance in the pain-related empathy task (TP). This suggests that the rIFG may be involved in understanding the meaning of pain through objective sensory cues. Consistent with this result, an imaging study by Budell et al. found that activity of the IFG was seen only when subjects were attending to the meaning of the pain expressions (Budell et al., 2010a; Budell et al., 2015). Another study also implied that the rIFG may be relatively more involved in encoding the semantic meaning features of gestures (Molnar-Szakacs, 2005; Straube, Green, Weis, & Kircher, 2012). The results in the present study, together with those of previous studies, indicated that the rIFG might be involved in coding pain through visual cues (not only facial expressions, but also sensory cues), which would enable the observer to infer another's state and would provide the neural basis for empathy for pain (Vachon-Presseau et al., 2012).

Additionally, we observed prolonged RTs during rTMS delivery to the rIFG under the painful condition, as compared with the control site, in the pain-related empathy task. Observed pain might be intimately linked with action systems. The sight of others in pain may imply the predicted collision between a noxious agent (i.e., the scissors' blade) and the human skin (i.e., a finger). This scene could present the observer with information about the potentially harmful outcome of touching the noxious object, which might facilitate motor responses aimed at avoiding or withdrawing from the noxious object. Morrison et al. provided evidence that witnessing pain in others could modulate the motor response in an observer to react quickly (Morrison, Peelen, & Downing, 2007). Behavioral studies by Galang et al. also found that participants responded faster after watching someone in pain. This response facilitation was further strengthened when participants were explicitly instructed to empathize with others' pain (Galang & Obhi, 2020). This motor response facilitation may be due to some survival instinct, as responding to threatening stimuli (e.g., pain or observed pain) quickly and efficiently would be highly beneficial. Some studies have suggested that this facilitatory mechanism might be modulated by the cingulate cortex and might promote the pain-related response (Calejesan, Kim, & Zhuo, 2000). In the present fMRI study, we indeed found that the rIFG showed significant functional connectivity with the middle cingulate cortex, which has been suggested to participate in empathetic processes (Keysers & Gazzola, 2014; Lamm et al., 2011a; Zaki & Ochsner, 2012). Consistent with this ecological interpretation, rTMS delivered to the rIFG site under the painful condition slowed the RT, implicating the rIFG in the swiftness of the behavioral response to other's pain. In this sense, activation of the rIFG might contribute to integrating and delivering perceptual and emotional motivation-related information to motor-related brain areas, where responses are prepared (Shamay-Tsoory, 2011; Shamay-Tsoory et al., 2009).

Moreover, the present rTMS experiment found a significant negative relationship between the behavioral results (adjusted RTs during stimulation of the rIFG in the pain-related empathy condition) and the trait cognitive empathy scores (measured by the FS subscale). This result seems inconsistent with our hypothesis that the rIFG is mainly involved in emotional empathy. In fact, whether the rIFG region is involved in emotional empathy or cognitive empathy remains controversial. A previous study found that higher scores of individual trait emotional empathy was associated with stronger activation in the rIFG (Lamm, Batson, & Decety, 2007). However, Massey et al. found that decreased cortical thickness of the rIFG was associated with worse performance in cognitive empathy tasks among individuals with schizophrenia (Massey et al., 2017). In line with these observations,

cognitive empathy necessitates the activity of the rIFG, as revealed by a recent tDCS brain stimulation study, and this tDCS effect is also negatively correlated with scores on the FS subscale (Wu et al., 2018). The FS subscale measures the tendency to transpose oneself into fictional situations imaginatively (Davis, 1983), which might also require emotional empathy representation of others (Schmidt et al., 2017). Furthermore, some scholars proposed that the hMNS system may be the infrastructure supporting empathy, and its activation is a prerequisite for emotional and cognitive empathy (Shamay-Tsoory, 2011; Shamay-Tsoory et al., 2009). As a core component of the hMNS, rIFG activity might be closely associated with both trait cognitive empathy and emotional empathy. It should be noted that the effect size was small in the correlation analysis and the significance did not survive Bonferroni correction. This may, in part, be due to the modest sample size. Future studies should employ larger samples in an attempt to validate our findings.

In conclusion, the fMRI findings of the present study replicated previous imaging evidence for the contribution of the rIFG (BA 45; the pars triangularis) to pain-related empathy processing. The novel findings of our study were that online rTMS of the rIFG can impair pain-related empathy processing. This TMS-induced effect might be modulated by individual trait cognitive empathy. To the best of our knowledge, no previous study had explored the role of the rIFG in pain-related empathy via TMS. These findings could have theoretical implications for understanding the basis of empathy and for clinical interventions in patients suffering from serious empathy disorders, as they provide data useful for the selection of sites for intervention and individualized intervention programs (as individual differences in trait empathy might constrain the efficacy of brain stimulation in specific areas).

## ACKNOWLEDGMENTS

This research was supported by grants from NSFC (61773092, 61673087, 61773096), Sichuan Science and Technology Program (2020YFS0230), 111 project (B12027), the Fundamental Research Funds for the Central Universities, Open Project of Sichuan Applied Psychology Research Center from Chengdu Medical College (CSXL-192A09), and Scientific Research of Sichuan Health Commission (19PJ193).

## CONFLICT OF INTEREST

The authors declare no conflicts of interest.

## DATA AVAILABILITY STATEMENT

The data that support the findings of this study are available from the corresponding author upon reasonable request.

## ORCID

*Ling Li* https://orcid.org/0000-0003-2471-0181

## REFERENCES

Adolfi, F., Couto, B., Richter, F., Decety, J., Lopez, J., Sigman, M., … Ibáñez, A. (2017). Convergence of interoception, emotion, and social cognition: A twofold fMRI meta-analysis and lesion approach. *Cortex*, *88*, 124–142.

Allen, M., Frank, D., Glen, J. C., Fardo, F., Callaghan, M. F., & Rees, G. (2017). Insula and somatosensory cortical myelination and iron markers underlie individual differences in empathy. *Scientific Reports*, *7* (43316), 1–12.

Bach, D. R., Flandin, G., Friston, K. J., & Dolan, R. J. (2010). Modelling event-related skin conductance responses. *International Journal of Psychophysiology*, *75*, 349–356.

Bernhardt, B. C., & Singer, T. (2012). The neural basis of empathy. *Annual Review of Neuroscience*, *35*, 1–23.

Betti, V., & Aglioti, S. M. (2016). Dynamic construction of the neural networks underpinning empathy for pain. *Neuroscience and Biobehavioral Reviews*, *63*, 191–206.

Beynel, L., Appelbaum, L. G., Luber, B., Crowell, C. A., Hilbig, S. A., Lim, W., … Deng, Z. D. (2019). Effects of online repetitive transcranial magnetic stimulation (rTMS) on cognitive processing: A meta-analysis and recommendations for future studies. *Neuroscience and Biobehavioral Reviews*, *107*, 47–58. https://doi.org/10.1016/j.neubiorev.2019.08.018

Bona, S., Herbert, A., Toneatto, C., Silvanto, J., & Cattaneo, Z. (2014). The causal role of the lateral occipital complex in visual mirror symmetry detection and grouping: An fMRI-guided TMS study. *Cortex*, *51*, 46–55.

Budell, L., Jackson, P., & Rainville, P. (2010). Brain responses to facial expressions of pain: Emotional or motor mirroring? *NeuroImage*, *53*, 355–363.

Budell, L., Kunz, M., Jackson, P. L., & Rainville, P. (2015). Mirroring pain in the brain: Emotional expression versus motor imitation. *PLoS One*, *10*, e0107526.

Bzdok, D., Schilbach, L., Vogeley, K., Schneider, K., Laird, A. R., Langner, R., & Eickhoff, S. B. (2012). Parsing the neural correlates of moral cognition: ALE meta-analysis on morality, theory of mind, and empathy. *Brain Structure & Function*, *217*, 783–796.

Calejesan, A. A., Kim, S. J., & Zhuo, M. (2000). Descending facilitatory modulation of a behavioral nociceptive response by stimulation in the adult rat anterior cingulate cortex. *European Journal of Pain*, *4*, 83–96.

Carrillo, M., Han, Y., Migliorati, F., Liu, M., Gazzola, V., & Keysers, C. (2019). Emotional Mirror neurons in the Rat's anterior cingulate cortex. *Current Biology*, *29*, 1301–1312.e6.

Chakrabarti, B., Bullmore, E., & Baron-Cohen, S. (2006). Empathizing with basic emotions: Common and discrete neural substrates. *Social Neuroscience*, *1*, 364–384.

Coll, M. P., Viding, E., Rütgen, M., Silani, G., Lamm, C., Catmur, C., & Bird, G. (2017). Are we really measuring empathy? Proposal for a new measurement framework. *Neuroscience and Biobehavioral Reviews*, *83*, 132–139.

Davis, M. (1980). A multidimensional approach to individual differences in empathy. *Journal of Chemical Information and Modeling*, *10*(85), 1–19.

Davis, M. H. (1983). Measuring individual differences in empathy: Evidence for a multidimensional approach. *Journal of Personality and Social Psychology*, *44*, 113–126.

De Waal, F. B. M., & Preston, S. D. (2017). Mammalian empathy: Behavioural manifestations and neural basis. *Nature Reviews Neuroscience*, *18*, 498–509.

Decety, J., & Lamm, C. (2006). Human empathy through the lens of social neuroscience. *TheScientificWorldJOURNAL*, *6*, 1146–1163.

Dimberg, U., Andréasson, P., & Thunberg, M. (2011). Emotional empathy and facial reactions to facial expressions. *Journal of Psychophysiology*, *25*(1), 26–31.

Dricu, M., & Frühholz, S. (2016). Perceiving emotional expressions in others: Activation likelihood estimation meta-analyses of explicit evaluation, passive perception and incidental perception of emotions. *Neuroscience and Biobehavioral Reviews*, *71*, 810–828. https://doi.org/10.1016/j.neubiorev.2016.10.020

Fan, Y., Duncan, N. W., de Greck, M., & Northoff, G. (2011). Is there a core neural network in empathy? An fMRI based quantitative meta-analysis. *Neuroscience and Biobehavioral Reviews*, *35*, 903–911.

Ferrari, C., Schiavi, S., & Cattaneo, Z. (2018). TMS over the superior temporal sulcus affects expressivity evaluation of portraits. *Cognitive, Affective, & Behavioral Neuroscience*, *18*, 1188–1197.

Filmer, H. L., Dux, P. E., & Mattingley, J. B. (2014). Applications of transcranial direct current stimulation for understanding brain function. *Trends in Neurosciences*, *37*, 742–753.

Forman, S. D., Cohen, J. D., Fitzgerald, M., Eddy, W. F., Mintun, M. A., & Noll, D. C. (1995). Improved assessment of significant activation in functional magnetic resonance imaging (fMRI): Use of a cluster-size threshold. *Magnetic Resonance in Medicine*, *33*, 636–647.

Friston, K. J., Frith, C. D., Turner, R., & Frackowiak, R. S. J. (1995). Characterizing evoked hemodynamics with fMRI. *NeuroImage*, *2*, 157–165.

Galang, C. M., & Obhi, S. S. (2020). Please empathize! Instructions to empathise strengthen response facilitation after pain observation. *Cognition and Emotion*, *34*, 316–328.

Gallese, V. (2007). Before and below "theory of mind": Embodied simulation and the neural correlates of social cognition. *Philosophical Transactions of the Royal Society, B: Biological Sciences*, *362*, 659–669.

Gallo, S., Paracampo, R., Müller-Pinzler, L., Severo, M. C., Blömer, L., Fernandes-Henriques, C., … Gazzola, V. (2018). The causal role of the somatosensory cortex in prosocial behaviour. *eLife*, *7*, 1–31.

Gao, X., Pan, W., Li, C., Weng, L., Yao, M., & Chen, A. (2017). Long-time exposure to violent video games does not show desensitization on empathy for pain: An fMRI study. *Frontiers in Psychology*, *8*, 1–10.

Grèzes, J., Armony, J. L., Rowe, J., & Passingham, R. E. (2003). Activations related to "mirror" and "canonical" neurones in the human brain: An fMRI study. *NeuroImage*, *18*, 928–937.

Gu, X., Eilam-Stock, T., Zhou, T., Anagnostou, E., Kolevzon, A., Soorya, L., … Fan, J. (2015). Autonomic and brain responses associated with empathy deficits in autism spectrum disorder. *Human Brain Mapping*, *36*, 3323–3338.

Gu, X., Liu, X., Van Dam, N. T., Hof, P. R., & Fan, J. (2013). Cognition-emotion integration in the anterior insular cortex. *Cerebral Cortex*, *23*, 20–27.

Hamzei, F., Vry, M. S., Saur, D., Glauche, V., Hoeren, M., Mader, I., … Rijntjes, M. (2016). The dual-loop model and the human Mirror neuron system: An exploratory combined fMRI and DTI study of the inferior frontal Gyrus. *Cerebral Cortex*, *26*, 2215–2224.

Hartwigsen, G., Neef, N. E., Camilleri, J. A., Margulies, D. S., & Eickhoff, S. B. (2019). Functional segregation of the right inferior frontal Gyrus: Evidence from Coactivation-based Parcellation. *Cerebral Cortex*, *29*, 1532–1546.

He, W., Fan, C., & Li, L. (2017). Transcranial magnetic stimulation reveals executive control dissociation in the rostral prefrontal cortex. *Frontiers in Human Neuroscience*, *11*, 1–8.

Hillis, A. E. (2014). Inability to empathize: Brain lesions that disrupt sharing and understanding another's emotions. *Brain*, *137*, 981–997.

Hutchison, W. D., Davis, K. D., Lozano, A. M., Tasker, R. R., & Dostrovsky, J. O. (1999). Pain-related neurons in the human cingulate cortex. *Nature Neuroscience*, *2*, 403–405.

Iacoboni, M. (2005). Neural mechanisms of imitation. *Current Opinion in Neurobiology*, *15*, 632–637.

Iacoboni, M. (2009). Imitation, empathy, and Mirror neurons. *Annual Review of Psychology*, *60*, 653–670.

Jabbi, M., Swart, M., & Keysers, C. (2007). Empathy for positive and negative emotions in the gustatory cortex. *NeuroImage*, *34*, 1744–1753.

Jackson, P. L., Meltzoff, A. N., & Decety, J. (2005). How do we perceive the pain of others? A window into the neural processes involved in empathy. *NeuroImage*, *24*, 771–779.

Jiang, Y., Hu, Y., Wang, Y., Zhou, N., Zhu, L., & Wang, K. (2014). Empathy and emotion recognition in patients with idiopathic generalized epilepsy. *Epilepsy & Behavior*, *37*, 139–144.

Jung, J., Bungert, A., Bowtell, R., & Jackson, S. R. (2016). Vertex stimulation as a control site for Transcranial magnetic stimulation: A concurrent TMS/fMRI study. *Brain Stimulation*, *9*, 58–64.

Kao, M.-H. (2014). Recent developments in optimal experimental designs for functional magnetic resonance imaging. *World Journal of Radiology*, *6*, 437.

Keeser, D., Meindl, T., Bor, J., Palm, U., Pogarell, O., Mulert, C., … Padberg, F. (2011). Prefrontal transcranial direct current stimulation changes connectivity of resting-state networks during fMRI. *The Journal of Neuroscience*, *31*, 15284–15293.

Keysers, C., & Gazzola, V. (2014). Dissociating the ability and propensity for empathy. *Trends in Cognitive Sciences*, *18*, 163–166. https://doi.org/10.1016/j.tics.2013.12.011

Lamm, C., Batson, C. D., & Decety, J. (2007). The neural substrate of human empathy: Effects of perspective-taking and cognitive appraisal. *Journal of Cognitive Neuroscience*, *19*, 42–58.

Lamm, C., Decety, J., & Singer, T. (2011). Meta-analytic evidence for common and distinct neural networks associated with directly experienced pain and empathy for pain. *NeuroImage*, *54*, 2492–2502. https://doi.org/10.1016/j.neuroimage.2010.10.014

Lamm, C., Rütgen, M., & Wagner, I. C. (2019). Imaging empathy and prosocial emotions. *Neuroscience Letters*, *693*, 49–53.

Liakakis, G., Nickel, J., & Seitz, R. J. (2011). Diversity of the inferior frontal gyrus-a meta-analysis of neuroimaging studies. *Behavioural Brain Research*, *225*, 341–347.

Loggia, M. L., Mogil, J. S., & Catherine Bushnell, M. (2008). Empathy hurts: Compassion for another increases both sensory and affective components of pain perception. *Pain*, *136*, 168–176.

Massey, S. H., Stern, D., Alden, E. C., Petersen, J. E., Cobia, D. J., Wang, L., … Smith, M. J. (2017). Cortical thickness of neural substrates supporting cognitive empathy in individuals with schizophrenia. *Schizophrenia Research*, *179*, 119–124.

McLaren, D. G., Ries, M. L., Xu, G., & Johnson, S. C. (2012). A generalized form of context-dependent psychophysiological interactions (gPPI): A comparison to standard approaches. *NeuroImage*, *61*, 1277–1286.

Molnar-Szakacs, I. (2005). The human mirror neuron system and nonverbal social communication: Action observation, imitation and gesture perception. *ProQuest Dissertations and Theses*, 1–134.

Morelli, S. A., Rameson, L. T., & Lieberman, M. D. (2014). The neural components of empathy: Predicting daily prosocial behavior. *Social Cognitive and Affective Neuroscience*, *9*, 39–47.

Morrison, I., Peelen, M. V., & Downing, P. E. (2007). The sight of others' pain modulates motor processing in human cingulate cortex. *Cerebral Cortex*, *17*, 2214–2222.

Pasalar, S., Ro, T., & Beauchamp, M. S. (2010). TMS of posterior parietal cortex disrupts visual tactile multisensory integration. *The European Journal of Neuroscience*, *31*, 1783–1790.

Preston, S. D., & de Waal, F. B. M. (2002). Empathy: Its ultimate and proximate bases. *The Behavioral and Brain Sciences*, *25*, 1–20.

Rymarczyk, K., Zurawski, Ł., Jankowiak-Siuda, K., & Szatkowska, I. (2016). Emotional empathy and facial mimicry for static and dynamic facial expressions of fear and disgust. *Frontiers in Psychology*, *7*, 1–11.

Saarela, M. V., Hlushchuk, Y., Williams, A. C. D. C., Schürmann, M., Kalso, E., & Hari, R. (2007). The compassionate brain: Humans detect intensity of pain from another's face. *Cerebral Cortex*, *17*, 230–237.

Schmidt, T., Roser, P., Ze, O., Juckel, G., Suchan, B., & Thoma, P. (2017). Cortical thickness and trait empathy in patients and people at high risk for alcohol use disorders. *Psychopharmacology*, *234*, 3521–3533.

Shackman, A. J., Salomons, T. V., Slagter, H. A., Fox, A. S., Winter, J. J., & Davidson, R. J. (2011). The integration of negative affect, pain and cognitive control in the cingulate cortex. *Nature Reviews Neuroscience*, *12*, 154–167.

Shamay-Tsoory, S. G. (2011). The neural bases for empathy. *The Neuroscientist*, *17*, 18–24.

Shamay-Tsoory, S. G., Aharon-Peretz, J., & Perry, D. (2009). Two systems for empathy: A double dissociation between emotional and cognitive empathy in inferior frontal gyrus versus ventromedial prefrontal lesions. *Brain*, *132*, 617–627.

Silva, C., Montant, M., Ponz, A., & Ziegler, J. C. (2012). Emotions in reading: Disgust, empathy and the contextual learning hypothesis. *Cognition*, *125*, 333–338.

Singer, T., Seymour, B., O'Doherty, J., Kaube, H., Dolan, R. J., & Frith, C. D. (2004). Empathy for pain involves the affective but not sensory components of pain. *Science (80- )*, *303*, 1157–1162.

Smallwood, R. F., Laird, A. R., Ramage, A. E., Parkinson, A. L., Lewis, J., Clauw, D. J., … Robin, D. A. (2013). Structural brain anomalies and chronic pain: A quantitative meta-analysis of gray matter volume. *The Journal of Pain*, *14*, 663–675.

Straube, B., Green, A., Weis, S., & Kircher, T. (2012). A Supramodal neural network for speech and gesture semantics: An fMRI study. *PLoS One*, *7*, e51207.

Timmers, I., Park, A. L., Fischer, M. D., Kronman, C. A., Heathcote, L. C., Hernandez, J. M., & Simons, L. E. (2018). Is empathy for pain unique in its neural correlates? A meta-analysis of neuroimaging studies of empathy. *Frontiers in Behavioral Neuroscience*, *12*, 1–12.

Vachon-Presseau, E., Roy, M., Martel, M. O., Albouy, G., Chen, J., Budell, L., … Rainville, P. (2012). Neural processing of sensory and emotional-communicative information associated with the perception of vicarious pain. *NeuroImage*, *63*, 54–62.

Valero-Cabré, A., Amengual, J. L., Stengel, C., Pascual-Leone, A., & Coubard, O. A. (2017). Transcranial magnetic stimulation in basic and clinical neuroscience: A comprehensive review of fundamental principles and novel insights. *Neuroscience and Biobehavioral Reviews*, *83*, 381–404.

World Medical Association. (2013). Declaration of Helsinki world medical association declaration of Helsinki. *Bulletin of the World Health Organization*, *79*, 373–374.

Wu, X., Xu, F., Chen, X., Wang, L., Huang, W., Wan, K., … Wang, K. (2018). The effect of high-definition transcranial direct current stimulation of the right inferior frontal gyrus on empathy in healthy individuals. *Frontiers in Human Neuroscience*, *12*, 1–12.

Yan, Y., Wei, R., Zhang, Q., Jin, Z., & Li, L. (2016). Differential roles of the dorsal prefrontal and posterior parietal cortices in visual search: A TMS study. *Scientific Reports*, *6*, 1–9.

Young, K. A., Gandevia, S. C., & Giummarra, M. J. (2017). Vicarious pain responders and emotion: Evidence for distress rather than mimicry. *Psychophysiology*, *54*, 1081–1095.

Zaki, J., & Ochsner, K. (2012). The neuroscience of empathy: Progress, pitfalls and promise. *Nature Neuroscience*, *15*, 675–680.

Zhang, F., Dong, Y., Wang, K., Zhan, Z., & Xie, L. (2010). Chinese version interpersonal reactivity index (IRI-C): A study of reliability and validity. *Chinese Journal of Clinical Psychology*, *18*, 155–157.

Zhang, Q., Wang, H., Luo, C., Zhang, J., Jin, Z., & Li, L. (2019). The neural basis of semantic cognition in mandarin Chinese: A combined fMRI and TMS study. *Human Brain Mapping*, *40*, 5412–5423.

## SUPPORTING INFORMATION

Additional supporting information may be found online in the Supporting Information section at the end of this article.

**How to cite this article:** Li Y, Li W, Zhang T, Zhang J, Jin Z, Li L. Probing the role of the right inferior frontal gyrus during Pain-Related empathy processing: Evidence from fMRI and TMS. *Hum Brain Mapp*. 2021;42:1518–1531. https://doi.org/10.1002/hbm.25310